Biomass gasification using low-temperature solar-driven steam supply

Zohreh Ravaghi-Ardebili [a], Flavio Manenti [a, *], Michele Corbetta [a], Carlo Pirola [b], Eliseo Ranzi [a]

[a] *Politecnico di Milano, Dipartimento di Chimica, Materiali e Ingegneria Chimica, "Giulio Natta", Piazza Leonardo da Vinci 32, 20133 Milano, Italy*
[b] *Università degli Studi di Milano, Dipartimento di Chimica, Via Golgi 19, 20133 Milano, Italy*

Received 9 January
2014 Accepted 14 July
2014 Available online

1. Introduction

Owing to oil price fluctuations, environmental protocols, and the significant growth in applying energy produced from non-fossil fuel sources, it is encouraging for the energy sector to focus the attention on the power generation from renewable-based power plants. On the other hand, saving energy and reducing fossil fuels consumption for high-consuming processes, such as coal-powered gasification processes, drives the attention to apply alternative sources for generating steam and energy with a strong insight on mechanistic physical and chemical aspects, in order to optimize power and chemical plants operation.

* Corresponding author. Tel.: +39 (0)2 2399 3273; fax: +39 (0)2 2399 3280.
E-*mail address:* flavio.manenti@polimi.it (F. Manenti).

Biomass gasification could provide a suitable way to produce syngas in a greener fashion, preserving a comparable efficiency with respect to traditional coal supplied gasifiers. Therefore, the focus on biomass is going to be concentrated intensively as a renewable source more than coal, and interests are driven towards sustainable bio-products for future, such as bio-methanol.

Several modeling and experimental studies focus the attention on biomass gasification to assess and evaluate the sensitivity of operating parameters on the efficiency of the process. [18] reported a lab-scale fixed bed reactor of steam biomass gasification considering the effect of particle size at different temperature above 700 °C. Results show that the efficiency of the gasification as well as the yield of hydrogen are increased by decreasing the particle size, consequently the content of char and tar decreases [18]. In the other interesting experimental study, [19] have reported the effect of air-steam gasification in a fluidized bed. They considered a series of operating parameters such as the ratio of steam to biomass (SBR),

equivalent ratio (ER), among the others, in different reactor temperatures, and they showed the direct effect of higher temperatures on higher hydrogen yield and the inverse effect on LHV [19]. [8,21] presented a very comprehensive work on the characteristic effect of the different biomass types on combustion [21]. Perez et al. studied the effect of operating and design parameters, especially the ge-ometry of the reactor, on the performance of the gasification/combustion of biomass in downdraft reactors [23]. The effect of air inlet temperature and oxygen concentration is analyzed by Ref. [30] as the gasifying agent in the updraft reactor [30].

The main objective of this work is to investigate the effect of different operating conditions and to design a new configuration of reactor for low-temperature gasification to achieve a compa-rable efficiency with respect to high-temperature gasification, looking for optimizing the molar ratio of H_2/CO in produced gas. The advantageous of this route relies on the possibility to use low-temperature steam derived from a renewable source of en-ergy (CSP plant), and simultaneously, preserving the calorific value of the process by manipulating the different effective operating parameters. Concentrated Solar Power plants are pro-posed in this work as an appropriate alternative to replace fossil fuels in providing low-temperature steam, fulfilling environ-mental and economic issues. According to the authors' knowl-edge, studies taking into account this aspect of study for low-temperature steam driven solar power plant biomass gasifica-tion for 2nd generation biofuels have not been published in the literature so far.

2. Steam and power generation

Steam is a critical energy vector and it is essential for all industrial processes for heating utilities, driving the equipment and powering the processes. Moreover, the dependency of the chemical industries from steam is inevitable and, therefore, it is promising to provide alternative clean productions of it. All conventional processes such as gas turbine combined cycle (CC), integrated gasification combined cycle (IGCC), pressurized fluidized bed combustion (PFBC) are fuel-based steam/power generation processes (see also [9,14]).

Nowadays, coal and natural gas are the main fuels to produce steam and power. Environmentally speaking, reducing the carbon footprint from the chemical plants requires the extensive attempts in reducing the energy requirement, and reducing the carbon emissions associated with the remaining energy is required [7,15,16]. In addition, changing the processes to one involving less energy-intensive chemistry route or less energy-intensive unit operations is the approach to reduce the consumption of energy by chemical industries. Moreover, changing the process to alter the relative requirements for thermal energy is the other approach for energy reducing purposes [32]. Following these approaches, replacing fuel-based power plants to renewable and clean source of energy could bring the beneficial challenging in comparison with the traditional ways of steam generation processes. In this work, it has been utilized the steam generated from a pre-designated concentrated solar power plant [33]. The process is accomplished based on storing the heated working fluid via solar collector field (Thermal Energy Storage, TES), and therefore, generating power. More details on solar plants and a comprehensive review on CSP technologies could be found in the work of [31].

3. Low-temperature biomass gasification

Biomass gasification is the thermo-chemical conversion of organic waste feedstock in a reduced oxygen medium (partial oxidization); while the combustion takes place completely in the presence of stoichiometric oxygen. The common operating temperature for gasification is rather high, commonly varies from 750 °C to 1000 °C, depending on the type of feedstock and oper-ating conditions. The resulting product is syngas, mainly composed by carbon monoxide, carbon dioxide, hydrogen, methane, and solid residues are the by-products (ashes and unconverted biomass). A relevant interest towards biomass gasification produced a huge number of scientific works and perspectives, which are nicely reviewed in the publication by Ref. [27]. Although the gasification is conceptually a high-temperature process, it might be operate at lower temperatures with adapting the effective parameters, operation conditions and alternative design options in the configuration of the reactor. The main concern of this activity is to investigate and apply the low-temperature steam (~410 °C) generated from the pre-designed solar power plant, which is integrated to the biomass gasification process and drives it efficiently (Fig. 1). According to the authors' knowledge, studies taking into account this aspect of study for low-temperature steam driven solar power plant biomass gasification for 2nd biofuels have not been published in the literature so far. [6] assess a solar-based electricity generation in Chile by CSP, achieved by a Solar Power Tower plant (SPT) using molten salt as heat carrier and store. [12] proposed a study on the gasification process for 3rd generation biofuels. In his work, the design is based on steam gasification of biomass with the heat directly provided by a solar concentrating tower, which provides temperatures over 1000 °C. However, in our work the low-temperature steam (~ 410 °C) is generated by the concentrated solar power plant and it provides the oxidizing agent for the gasification process.

In order to provide the consistent and effective operation, the process is controlled by thermochemical heat of reaction along with related key parameters. Due to the applications of the product syngas, which could be used as a fuel, or to produce chemicals, it is crucial to keep high the yield of hydrogen and carbon monoxide, thus reducing the amount of unconverted solid residue. In addition, when the final goal is the synthesis of chemicals, such as methanol or dimethyl ether, it would be appropriate to keep controlled the molar ratio of H_2/CO (close to the value of two for methanol synthesis). In order to demonstrate the process feasibility of low-temperature steam biomass gasification, it is necessary to understand and unveil the chemistry involved in the process, in order to design an effective solar-powered gasifier. Fig. 2 shows the schematic of the gasifier, underlining the multi-scale nature of the process. The process is modeled starting from the description of the chemical evolution of biomass particles, which are discretized into concentric shells. Solid particles interact with the surrounding gas phase, which is considered as perfectly mixed. Several gas−solid elemental layers could be then interconnected in a cascade to reproduce the updraft gasifier at the reactor scale.

In the detailed chemical description, the process occurs in the three main stages. Drying happens around 100 °C, releasing water vapor from the surface and inner pores of the solid fuels. In this stage, some organic and inorganic compounds of fuel are released. Pyrolysis, which is observed by increasing the temperature, is a transient step to promote the destructuring of the solid fuel, originating new chemical species. Three main products derives from this stage and are usually classified in light gases, tars and char. The gasification and combustion stage, which includes the main gas−solid reactions, occurs between the solid fuel (char) and the chemical species in the surrounding atmosphere. The gaseous species include these released during drying and pyrolysis. Moreover, hot ashes and unconverted char are responsible for the heating of the oxidizing gas fed from the bottom. In comparison, combustion process requires the use of stoichiometric oxygen, which might produce H_2O, CO_2, related to the fuel compositions.

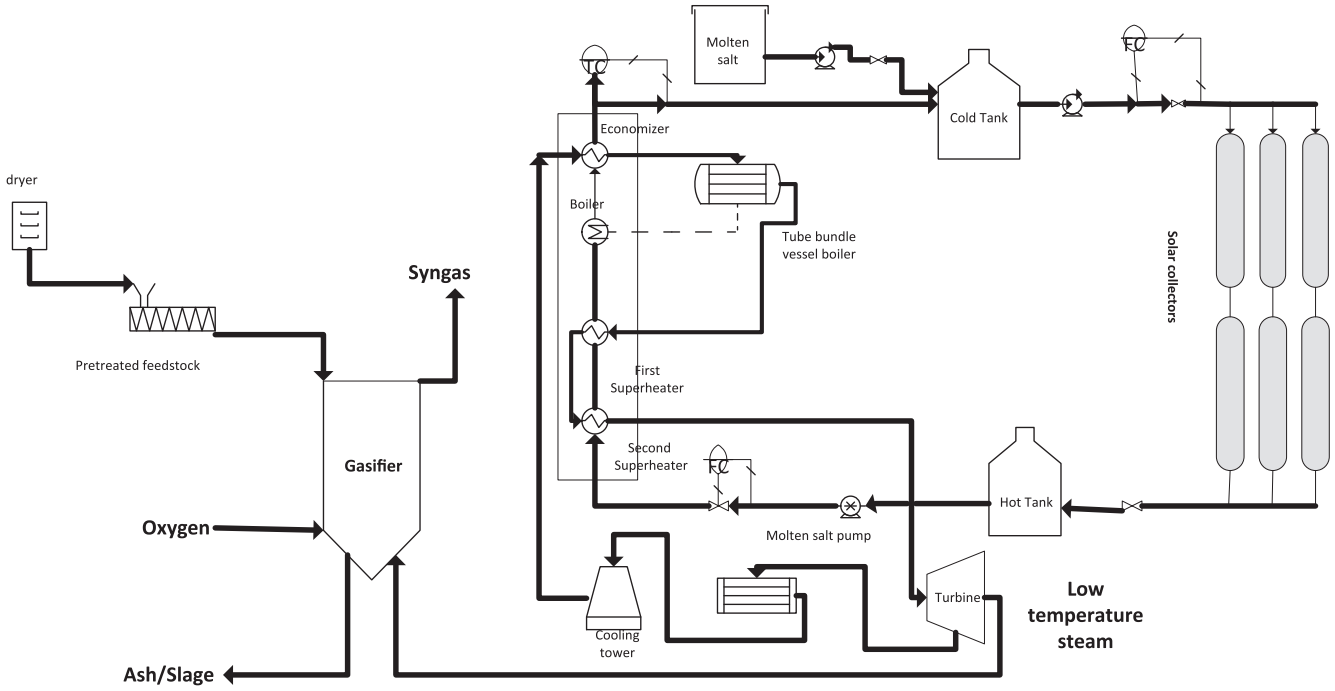

Fig. 1. The integrated biomass gasification with CSP plant.

Though the gasification by the use of steam or oxygen as reactant originate a more complex mixture, including CO, H_2, CO_2, CH_4, H_2O [1,2]. Controlling the process by the relevant operating conditions and parameters is going to be discussed in next section. Therefore, by supporting steam from a sustainable process (CSP plant), the gasification process would be independent of the co-fuel powered process (natural gas or coal). The two critical steps for a better understanding of biomass thermochemical conversion are the development of mechanistic models capable of describing transport phenomena and reaction kinetics together with the integration of these models at the process scale to approach novel process solutions. For the former step, detailed chemical mechanisms are needed both for biomass pyrolysis and for the successive gas phase reactions, since they are still unavailable even for major products released such as levoglucosan, hydroxymethylfurfural, and phenolic species [26]. Chemical mechanisms need to be integrated into particle models accounting for transport phenomena, which are critical in predicting global reactor performance. Developing these models is challenging because of the biomass complexity as well as the multi-phase and multi-scale nature of the

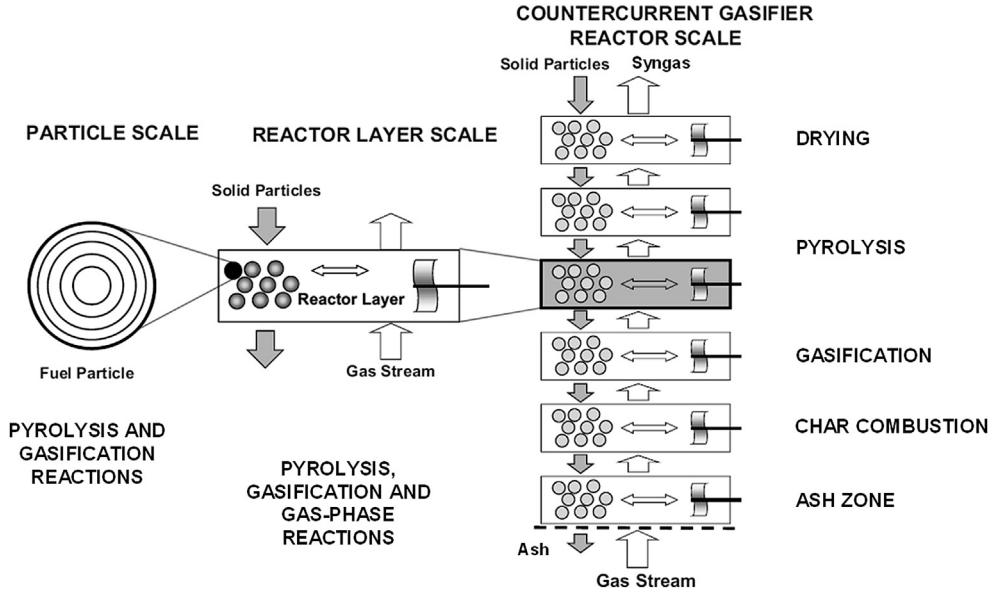

Fig. 2. Comprehensive schematic of gasification and interaction of solid–gas phase in each layer.

Table 1
The general comparative conditions in different fixed bed gasifiers [13].

Gasifier	Updraft (Counter-current)	Downdraft (Co-current)	Crossdraft
Size of the particle (mm)	Up to 100	5–100	1–3
Content of moisture (%)	<25	<60	<12
Ash content (%)	<6	<25	<20

conversion process [20]. For the latter step, the pre-designed two-tank direct thermal energy storage of CSP plant is linked to the gasification process.

4. Results and discussion

In order to re-design the gasifier coupled with the low-temperature solar driven steam, a sensitivity analysis is per-formed on the key operative parameters, which are the humidity of the feedstock, the size of the solid particles, the equivalent ratio, the steam to biomass ratio, and the residence time by changing reactor volume or inlet flowrates. Due to this, the comprehensive modeling package for the solution of multi-scale problems involving gas and solid interactions, so-called GASDS (Gas And Solid Dynamic Simulator [26], has been used to model and simulate the gasification process. The package includes the above-mentioned kinetic schemes as well as particle and reactor models. GASDS is able to solve the mass and energy balances accounting for reaction kinetics along with transport phenomena, by estimating the transport properties considering the morphological changes occurring during the pyrolysis and gasification process. Moreover, the model is capable to predict the solid and gas phase temperature profiles, product solid and gas phase compositions, amount of residual char, and so on. Modeling details are provided in Appendix A.

4.1. Gasifier configuration

The design and type of the gasifier depends on the quality and quantity of the feedstock, the position of the entrance of solid feedstock and throughputs leaving out the gasifier. Generally, the oxidizing agents are air/oxygen, steam and CO_2 to accomplish the gasification. Fixed bed reactor is the most applicable configuration for the biomass gasification, and it is classified into three main categories: downdraft (co-current), updraft (counter-current), and crossdraft (cross-current) [13]. The significant parameter to select the configuration of gasifier in fixed bed reactor is mentioned to determine the adaptive gasifier (Table 1).

Counter-current configuration is the classical design for gasifiers. Typically, in the updraft reactor, the biomass is fed in at the top of the reactor and moves downwards because of its conversion and the removal of ashes through a grate at the bottom of the reactor [22]. It is more widespread owing to its configuration and the lower temperatures of the leaving gas from the top of the gasifier, and, as a results, higher efficiency of the produced gases, less sensitivity to the moisture content (up to 25%), and size of the particle [3]. The gasification agent enters at the bottom below the grate and diffuses up through the bed of biomass and char; the flue gas leaves at the top of reactor. The agent enters from the bottom is in direct contact with hot ash in the bottom and un-converted char dropping down. Therefore, the exceeded temper-ature of wall in the bottom increases the ignition temperature of carbon, while, in downdraft reactor, the direction of contact be-tween solid and gas is towards down (co-current). Consequently, the reaction regions inside the reactor are different from of the updraft ones. In addition, the temperature regime displays inverse performance, where the hot gas moves downwards over the remaining hot char and it causes the tar free low energy content gases [2]. Heat necessary to carry on endothermic pyrolysis and gasification reactions could be provided by the heat of char combustion, thus enhancing the rate of reactions as a catalyst. The major advantages of this type of gasifier are its simplicity in design, high degree of controllability, high charcoal burn-out and internal heat exchange leading to low gas exit temperatures and high gasification efficiencies. Due to the internal heat exchange structure, the fuel is dried at the top of the gasifier and therefore fuels with high moisture content can be used (up to 50% wt.) [14].

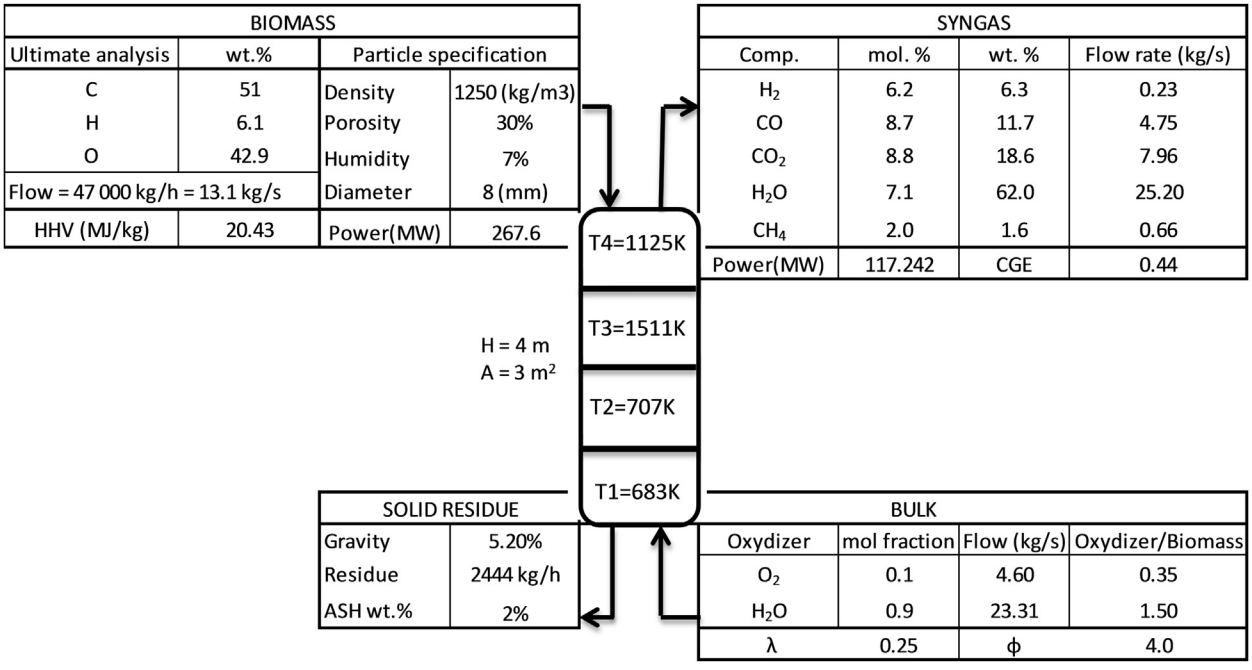

Fig. 3. The operating condition for low-temperature steam biomass gasification (solar driven steam at 683 K = 410 °C).

Table 2
Compositions of the two modeled biomass feedstock.

Component (% wt.)	Cellulose	Hemicellulose	Lignin C[a]	Lignin H[a]	Lignin O[a]	Ash
Cellulose-based biomass	40	20	5	25	8	2
Lignobiomass	35	8	30	20	5	2

[a] Lignin C, Lignin H and Lignin O represent their characteristic of being richer in carbon, hydrogen, and oxygen, respectively [25].

4.2. Sensitivity analysis on operating conditions

This overall process is modeled according to the following primary operating and characteristic conditions (base case) (Fig. 3). The successive changes on parameters would occur moving from the under discussed operating conditions. A common lignocellulosic biomass has been adopted with a cellulose amount of 40 wt. % and 2 wt. % of ashes. The elemental analysis of the biomass feedstock is presented in Fig. 3, based on C, H and O content.

4.2.1. The effect of biomass composition

Although the chemistry of biomass gasification is complex, it needs to specify some adequate and comprehensive kinetics to understand the process. Due to this, it is essential to identify and characterize the key components of biomass. A simplified description of biomass composition is usually given in terms of proximate analysis (moisture, ash, fixed carbon, and volatile matters), elemental analysis (C, H, S, N, and O), or biochemical analysis (cellulose, hemicellulose, and lignin, together with extractives, in either water and ethanol or toluene) [10]. With the biochemical analysis, the composition of biomass might be indicated directly in terms of cellulose, hemicelluloses, lignin, moisture, and either ash content. Although, biomass is benefited from the high content of oxygen in its structure and it does need less oxygen to add for gasification process, it should be noticed that this feature causes a relatively low calorific value of gasification in comparison with gasification of coal [24]. As it was discussed earlier, the three main component of biomass are well known in general as cellulose, hemicellulose and lignin. Lignin is a highly cross-linked polymer of methoxy- and phenoxy-sunstitiuted phenyl propane units. Cellulose is a complex polymer of glucose while different sugar units compose hemicellulose. Lignin generally has lower oxygen and higher carbon compared to those two others. In this section, it has been tried to discover the sensitivity of syngas quality on the composition of the biomass feedstock. In order to this, the gasification of two general kind of biomass has been simulated, as it is shown in Table 2. The first one is called cellulose-base biomass and it is the common lignocellulosic biomass, with a content of cellulose dominant and higher than the other two constitutes (i.e. lignin and hemicellulose). The other type of biomass, titled lignin base biomass, is a biomass rich in lignin. It is worth to mention that this kind of lignobiomass could derive from 2nd generation biorefineries as a by-product. Primary conversion processes (generally pre-treatment and hydrolysis) are able to break down virgin biomass into cellulose, hemicellulose and lignin. After this separation, C_5 and C_6 sugars are usually subjected to fermentation and/or solid-catalyzed processes, while lignin represents a by-product that can be interestingly converted to syngas.

Regarding to biomass type, it is demonstrated that if the biomass has higher content of lignin (lignin base biomass), it results in higher values of the H_2/CO molar ratio in comparison with the cellulose-based biomass. It is proven by the higher content of carbon in lignin base biomass, which gives a higher ratio of hydrogen to CO, as the behavior of coal based feedstock (Figs. 4 and 5).

4.2.2. The effect of moisture content

The moisture in the structure of the fuel has undesirable effects on gasification process. Since higher amounts of moisture in solid

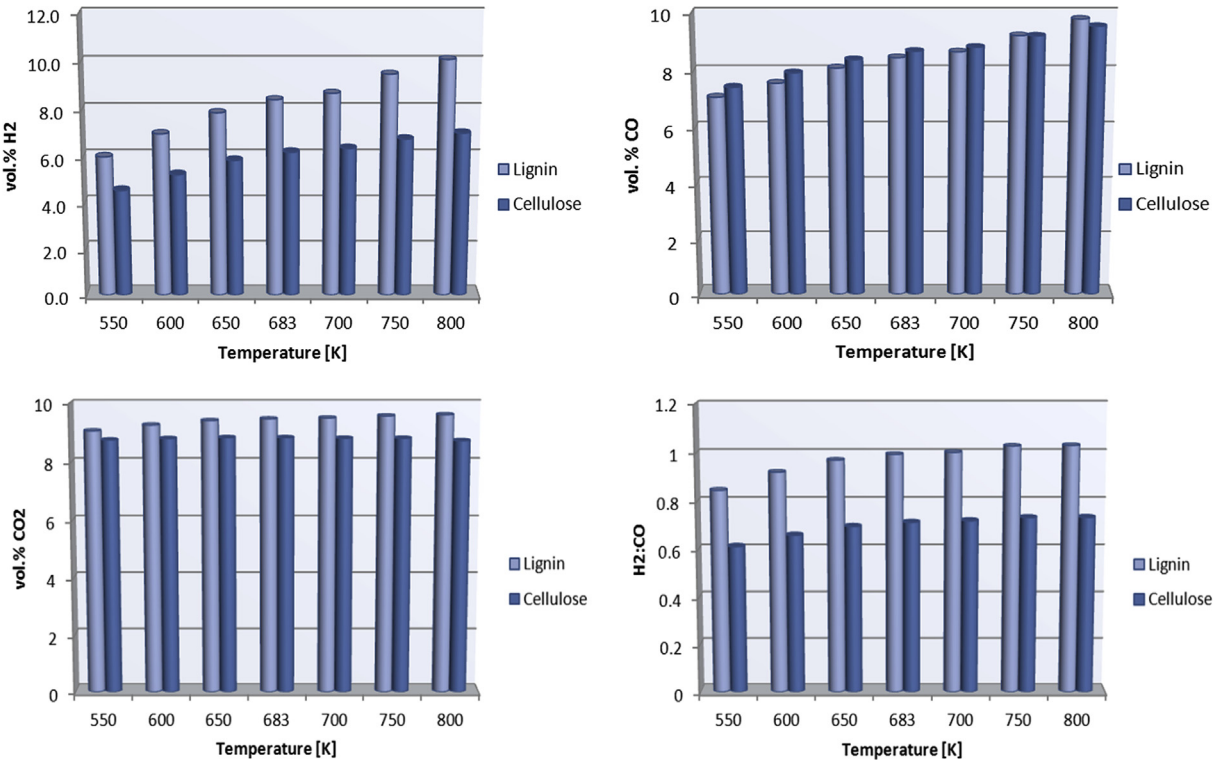

Fig. 4. The composition of the produced gases in low-temperature gasification based on the type of feedstock and H_2/CO molar ratio.

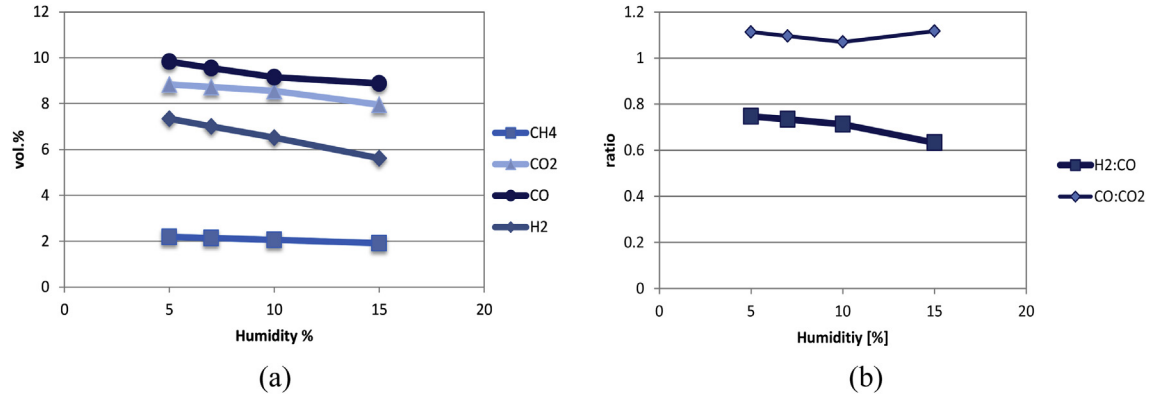

Fig. 5. a) The effect of the humidity on syngas production, and b) CO/CO_2 and H_2/CO molar ratios ($T = 800$ K).

fuels absorb energy and result in decreasing the temperature of gasification, which causes a less efficient process. Biomass has high moisture contents in its structure in addition to other components. Therefore, it is necessary to reasonably decrease the content of water, especially in the case of low-temperature gasification. Thus, the pretreatment process is required to dry the feedstock before feeding it into the gasifier. Although, drying is an energy-intensive pretreatment process, it provides considerably benefits for combustion and gasification compared to the initial raw state such as increased boiler efficiency, lower fuel gas emissions, and improved operations in utilities [11,17]. The content of water in feedstock could affect the efficiency of the process and decrease the yield of produced syngas. Therefore, it needs to be pretreated and dried before applying as feedstock. As it could be seen from the molar ratio of H_2/CO, the complete drying pro-cess is not necessary as contents of moisture less than 10% provide the same efficiency (Fig. 6b). Therefore, a moderate humidity around 7% is sufficient for an acceptable process, as it is applied in this work. Besides, the higher content of moisture in feedstock might provide the incomplete combustion and cause the less ef-ficiency in the process. To compensate the energy consumed in the process, it would be useful to integrate the heat for drying with other units.

Different amounts of moisture spanning from 5 to 15% (Fig. 5a) show that at higher amount of humidity, the yield of the flue gases decrease sharply. Therefore, drying as pretreatment process for biomass is important especially in low-temperature gasification where the yield of syngas is strongly sensitive to the operative parameters.

4.2.3. The effect of particle size

It has been tried to investigate and predict the effect of the size of biomass particles on H_2/CO molar ratio. In order to this, two different sizes, lower than 1 cm (5 mm) and higher (2 cm), have been selected for general conclusions (Fig. 6).

The smaller size of the particle is under control of kinetics, while heat and mass transfer limitations on the surface of the particle affect the larger size. In other words, by growing the size of particles, the heat transfer resistance in the radial direction of the particle increases, and therefore, the temperature of inner sectors are not high enough to complete the pyrolysis and the gasification reactions, and hence, fewer yields of hydrogen and the other species are observed (Fig. 7a). The molar ratio of H_2/CO is resulted 0.83 and 0.55 for 5 mm and 5 cm, respectively. In addition, the content of solid residue is reported 4.66 wt. % and 11.81 wt. % for 5 mm and 2 cm, respectively. By this, it could be resulted that although decreasing the size of particles does not significantly affect the content of the produced gas, the remarkable effect of it on efficiency and complete gasification, and the lesser amount of solid residues should be taken into account.

4.2.4. The effect of equivalent ratio

Fuel-Air Equivalence Ratio (ER) is defined as the actual fuel to oxygen ratio divided by the stoichiometric fuel to oxygen ratio [4,28], while Air-Fuel Equivalence ratio (λ) is the reciprocal of ER.

As it can be seen from Fig. 8, the trend of the final solid residue obviously decreases by increasing the temperature, due to the speed-up of kinetics (Fig. 8a). Moreover, increasing the percentage of oxygen (i.e. increasing λ or decreasing ER), the final solid residue

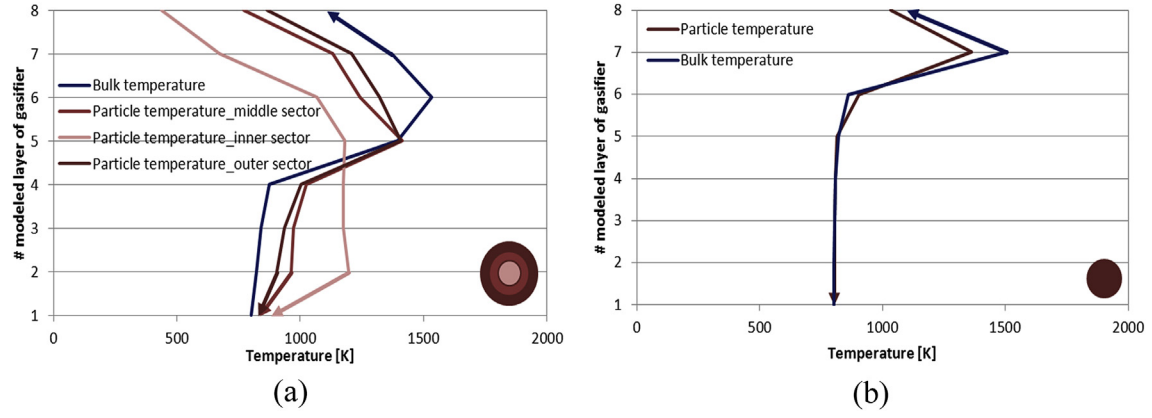

Fig. 6. Temperature profile of bulk and particle in modeled gasifier in terms of layer: a) particle size: 2 cm, and b) particle size: 5 mm.

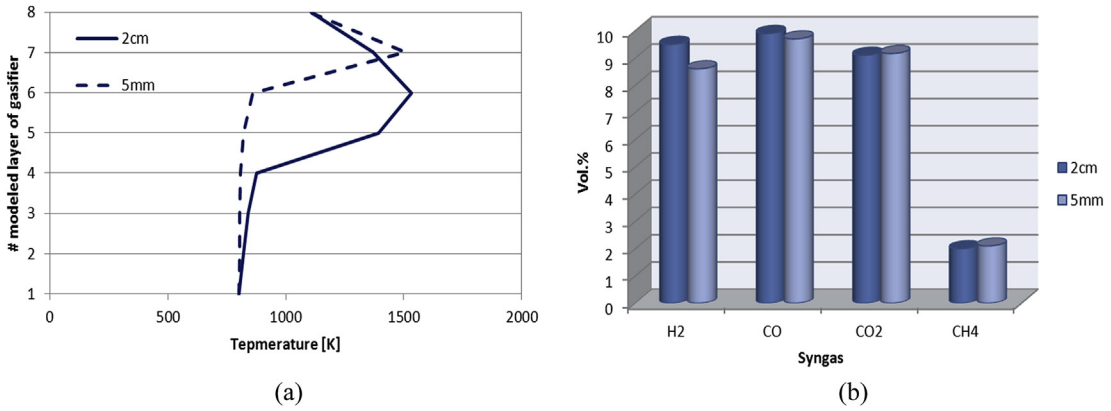

Fig. 7. a) The temperature profile of gas phase, and b) the composition of produced gases in two different sizes of particle.

decreases as well, due to the higher availability of the oxidant agent. Concerning the quality of the produced syngas, decreasing ER (or increasing λ) increases the molar ratio of H_2/CO, as it can be seen in Fig. 8b. Increasing the temperature increases the ratio as well. The optimum amount of oxygen is found at $\lambda = 0.25$ (i.e. ER = 4) for the target temperature of 700 K as it is highlighted in Fig. 8. These conditions present 6.5 wt. % of solid residue. It is worth noting that at lower λ at 600 K, the yield of H_2 abruptly decreases because the temperature is extremely low and causes the undesired shut down of the process.

The significant result, is the high value of residue production at $\lambda = 0.2$ and 700 K, which shows that gasification is incomplete. By increasing the amount of actual oxygen, lesser content of residue is observed, which means a more efficient gasification.

4.2.5. *The effect of residence time*

Residence time is one of the key parameters affecting the efficiency of the gasification process. According to the intrinsic multiphase nature of the process, it is necessary to provide enough residence time for the bulk and biomass particles to accomplish the relative gas–solid interactions and thermochemical reactions.

According to the inverse relationship of residence time and the flowrate of the feedstock, increasing the flowrate, keeping constant the volume of the gasifier, would decrease the residence time for reactions and this would cause inefficient gasification and consequently, increased amount of residue in the production. As it is shown in Fig. 9a, this effect is more intensive in lower temperature, while at higher temperature this effect is not as sensitive as the lower temperature. As a result, by increasing the residence time inside the gasifier, the efficiency of the process and the molar ratio H_2/CO increases. Indeed, this increased value is higher for the high-temperature operation than of for lower-temperature operating conditions. As the desired temperature for this activity is around 700 K, it is found an average ratio around 0.8 (Fig. 9b).

4.3. *Redesigning the low-temperature gasifier with economic evaluation*

Decreasing solid residue as a benchmark of efficiency in low-temperature gasification motivates the concept of re-designing the solar driven gasifier, operating in the range of temperatures between 683 K and 700 K, at similar operating conditions. Two different cases are selected for decreasing the content of final residue by varying the amount of oxygen supported to the gasifier in the first case, and increasing the height (volume) of the reactor in the second case. As it is obvious, by increasing the amount of oxygen in the plant, as it has been discussed in above-sections, the efficiency of the gasification is increased (CASE A). In addition, providing more residence time for biomass particles by increasing the volume of the gasifier with identical operating conditions (such as the flowrate of feedstock), would meet the efficiency of the gasification process (CASE B). In order to this, we tried to model both situation with considering the economic evaluation for each proposed case, and therefore, the proper decision making to re-design the low-temperature gasifier with respect to the discussed

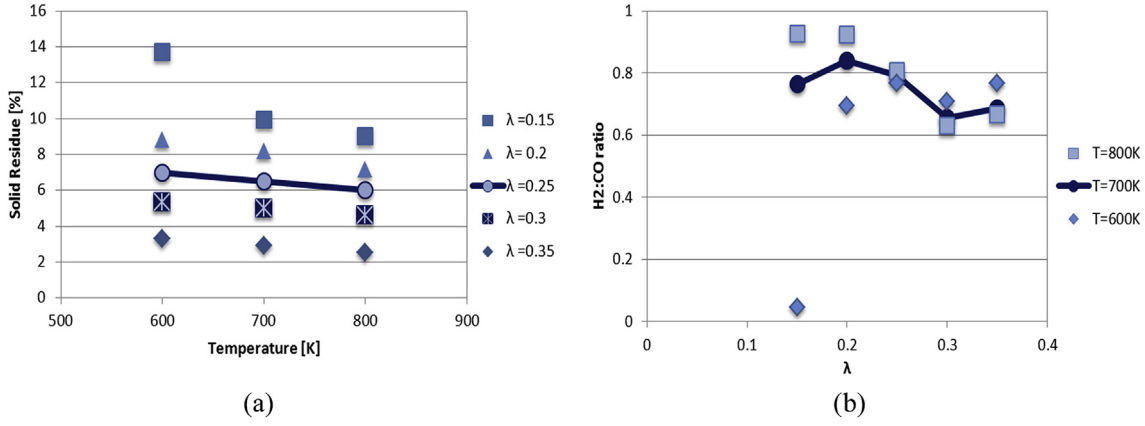

Fig. 8. The effect of ER on lower-temperature gasification (SBR = 1.2): a) effect on final solid residue [wt. %], and b) effect on H_2/CO molar ratio.

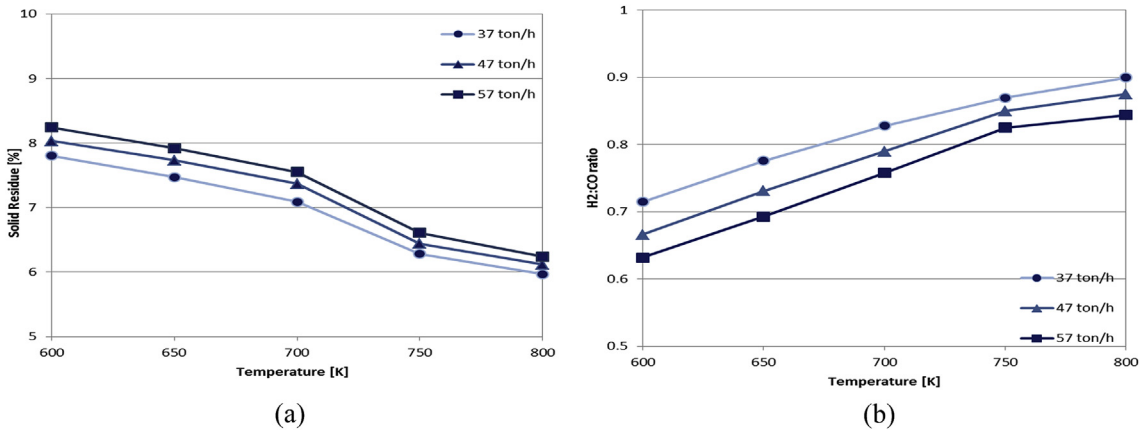

Fig. 9. The effect of residence time on lower-temperature gasification: a) effect on residue in production, and b) effect on H_2/CO ratio.

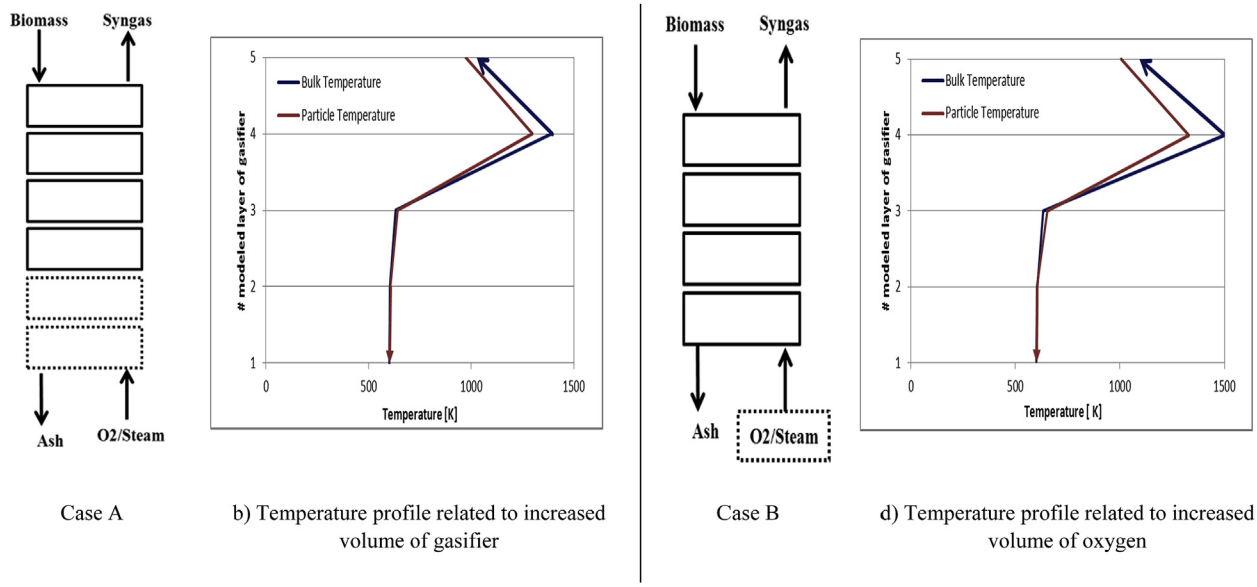

Fig. 10. Decision making to Re-design the low-temperature gasification process a) increased height of reactor, and, c) increased oxygen injected.

operating conditions. Due to this, the performance of these cases is evaluated for 1 wt. % decreasing in amount of solid residue.

As it is obvious from Fig. 10, by increasing the height of gasifier, that it means increasing the residence time for the identical flowrate of feedstock, the efficiency of the process is higher in comparison with the lower height of reactor. This decreased amount of residue (−1 wt. %) occurs at 2 m promoting the height. However, in CASE B, this happens for 0.288-increased amount of oxygen (Nm^3/s) in comparison with base operating condition. The feedstock flowrate is kept constant at 47,000 kg/h for both cases.

The calculated capital costs and cost of oxygen are presented in Table 3. It is obviously observed that the cost for supplying the extra oxygen to the plant is yearly 13.7 times the capital cost of replacing a larger gasifier to the plant. This result highlights the importance of carefully designing the gasifier instead of changing the operative parameters to increase the efficiency of the process and meet the desired requirements.

5. Conclusions

A low-temperature steam generated by concentrated solar power plant is coupled to biomass gasification. The study is targeted to investigate and demonstrate the efficiency of low-temperature biomass gasification. Due to this, the effective operating and pretreatment parameters are considered along with their effect on H_2/CO molar ratio and composition of syngas. In addition, the work

Table 3
Re-design of the gasifier.

	Oxygen cost ($/mol)	Gasifier cost ($/$m^3$)	Reference cost estimation Eq.	Cost per 1 wt. % decreased residue ($/year)	Reference year
Case A	0.07	–	–	616,999	2010
Case B	–	15000	[b] C_2=C1.$(S_1/S_2)^{0.6}$	44,862.5	2004[a] [29]

[a] The cost is correlated according to "cost (year 2012) = cost (year 2004). (CI_{2010}/CI_{2004})".
[b] S_1 and S_2 are the size of equipment, C_1 and C_2 are the rapid capital costs [29].

shows which is the best way to increase the efficiency of the process. The re-designing of the gasifier (in order to change the residence time) was compared with the increasing of the oxygen injected to the reactor, and, according to the cost analysis, it results that oper-ational investment for increasing of the oxygen flowrate is 13.7 times more than re-designing the gasifier (installation investment).

Appendix A. GASDS: a multi-scale, multi-phase dynamic simulator

Intra- and inter-phase heat and mass transfer phenomena need to be considered and coupled with the kinetics when modeling reactors treating thick particles. According to prior works [26], a convenient way to present the mass and energy balance equations is to distinguish the particle and the reactor scale as implemented in the GASDS tool. Soon an evolution of this tool, the FLOGA Suite, will be also available at the website super.chem.polimi.it.

A.1. The particle scale

The particle model should be able to predict temperature profiles and species distribution as a function of time. This model requires not only reaction kinetics, but also reliable rules for estimating transport properties to account for morphological changes during the pyrolysis process. Biomass particles shrink by as much as 50% during their conversion. Heat transfer must account for variable transport properties during the pyrolysis process: namely, in virgin biomass, dry and reacting biomass, and the re-sidual char.

The intra-particle mass and heat transfer resistances are characterized by assuming an isotropic sphere. The particle is discretized into several sectors to characterize temperature and concentration profiles as well as the dynamic behavior of the particle under different regimes (pyrolysis, gasification and combustion). The gradients of temperature and volatile species inside the particle are evaluated by means of the energy and continuity equations, respectively. N sectors are assumed to discretize the particle. The mass balance of the solid phase is:

$$\frac{\mathrm{d}m_{j,i}}{\mathrm{d}t} = V_j R_{j,i} \tag{1}$$

where $m_{j,i}$ is the mass of the ith solid component; V_j is the volume of the jth sector; $R_{j,i}$ is the net formation rate of the ith component resulting from the multi-step devolatilization model and from the heterogeneous gas–solid reactions in the jth sector; finally, t is the time variable.

The mass balance of the gas phase is:

$$\frac{\mathrm{d}m_{j,i}}{\mathrm{d}t} = J_{j-1,i}S_{j-1} - J_{j,i}S_j + V_j R_{j,i} \tag{2}$$

where $m_{j,i}$ is the mass of the ith volatile species within the jth sector; S_j is the external surface of the jth sector; and J are the total fluxes generated by diffusion and pressure gradients.

The energy balance is:

$$\frac{\mathrm{d}\sum_{i=1}^{\mathrm{NCP}} m_{j,i}h_{j,i}}{\mathrm{d}t} = JC_{j-1}S_{j-1} - JC_jS_j + S_{j-1}\sum_{i=1}^{\mathrm{NCG}} J_{j-1,i}h_{j-1,i} - S_j\sum_{i=1}^{\mathrm{NCG}} J_{j,i}h_{j,i} + V_j HR_j \tag{3}$$

where $h_{j,i} = c_{P_{j,i}}T_j$ is the component partial enthalpy; T_j is the temperature of the jth sector. The term JC accounts for the heat conduction; the term $V\cdot HR$ accounts for the total reaction heat; NCP is the total number of components; and NCP is the number of gas components.

Mass exchange between adjacent sectors is only allowed for the volatile species, whereas solid compounds are constrained to remain inside the sector. The density profile inside the particle is evaluated as the sum of all the densities of different species $m_{j,i}$ present in each sector. Similarly, the shrinking and porosity of each sector are calculated. Mass and heat fluxes within the particle follow the constitutive Fick, Fourier, and Darcy laws:

$$J_{j,i} = -D_{j,i}^{\mathrm{eff}} MW_i \left.\frac{\mathrm{d}c_{j,i}}{\mathrm{d}r}\right|_{r_j} - \frac{Da_j}{\mu_j}\left.\frac{\mathrm{d}P_j}{\mathrm{d}r}\right|_{r_j} c_{j,i}MW_i \tag{4}$$

where $D_{j,i}^{\mathrm{eff}}$ is the effective diffusion coefficient of the $i-$th component inside the jth sector; MW and c are the molecular weight and the concentration; r is the radius; Da is the Darcy coefficient of the solid; μ is the viscosity of the gas phase; P is the pressure.

$$JC_j = -\kappa_j^{\mathrm{eff}}\left.\frac{\mathrm{d}T_j}{\mathrm{d}r}\right|_{r_j} \tag{5}$$

where κ_j^{eff} is the effective conduction coefficient inside the jth sector.

The boundary conditions at the gas–solid interface become:

$$J_{N,i} = k_{\mathrm{ext}}MW_i\left(c_{N,i} - c_i^{\mathrm{bulk}}\right) + \left.\frac{Da_N}{\mu_N}\frac{\Delta P}{\Delta r}\right|_N c_{N,i}MW_i \tag{6}$$

$$JC_N = h_{\mathrm{ext}}\left(T_N - T^{\mathrm{bulk}}\right) + JR_N + \sum_i^{\mathrm{NCG}} J_{N,i}h_{N,i} \tag{7}$$

where k_{ext} and h_{ext} are the convective transfer coefficients [34] and JR_N is the net radiation heat.

A.2. Reactor scale

While the mathematical model of fluidized bed or entrained bed reactors can directly refer to the previous particle model, the modeling of fixed bed reactors takes advantage from the definition of an elemental reactor layer describing the gas–solid interactions. The solid bed is then simulated as a series of NR elemental layers, as reported in Fig. 2. The height of each layer is of the same order of the size of the biomass particle, accounting for the vertical dispersion phenomena. The complete mixing inside the layer both for the gas and solid phase is assumed. In fact, the mixing of the main gas flow is further increased because of the energy provided by the volatile species released from the particles during the biomass pyrolysis.

The gas phase mass balance equations for each elemental reactor are:

$$\frac{\mathrm{d}g_i}{\mathrm{d}t} = G_{\mathrm{in},i} - G_{\mathrm{out},i} + J_{N,i}S_N\eta + V_R R_{g,i} \tag{8}$$

where g_i is the mass of the ith species within the reactor volume V_R; $G_{\mathrm{in},i}$ and $G_{\mathrm{out},i}$ are the inlet and outlet flowrate; $R_{g,i}$ is the net formation from gas-phase reactions; the term $J_{N,i}$ is the gas–solid mass exchange multiplied by the particle surface S_N and the number η of particles inside the layer.

The gas-phase energy balance equation for each elemental reactor is:

$$\frac{\mathrm{d}\sum_{i=1}^{\mathrm{NCG}} g_i h_{g_i}}{\mathrm{d}t} = \sum_{i=1}^{\mathrm{NCG}} G_{\mathrm{in},i} h_{g_{\mathrm{in},i}} - \sum_{i=1}^{\mathrm{NCG}} G_{\mathrm{out},i} h_{g_i} + \sum_{i=1}^{\mathrm{NCG}} J_{N,i} h_{N,i} S_N \eta + h_{\mathrm{ext}}\left(T_N - T^{\mathrm{bulk}}\right) S_N \eta + V_R H R_g \tag{9}$$

where $h_{g,i} = c_{P_i} T^{\mathrm{bulk}}$; T^{bulk} is the gas phase temperature; the terms $G \cdot h_g$ are the enthalpies of inlet and outlet flowrates; the term $J \cdot h$ is the enthalpy flux relating to the mass transfer of a single particle; finally HR_g is the overall heat of gas phase reactions.

As a matter of simplicity, the reactor index (from 1 to NR) is not reported in the balance equations (8) and (9). Fig. 2 highlights the interactions between adjacent reactor layers, while further boundary conditions and closure equations are needed to characterize different reactor configurations. Numerical methods and the structure of the Jacobian matrix are discussed in Ref. [26] and in Ref. [5].

References

[1] Badeau JP, Levi A. Biomass gasification: chemistry, process and application. Nova Science Publisher; 2009. ISBN: 978-1-61122-683-6.

[2] Basu P. Biomass gasification and pyrolysis. Elsevier; 2010. ISBN: 978-0-12-374988-8.

[3] Beenackers AACM. Biomass gasification in moving beds, a review of European technologies. Renew Energy 1999;16:1180–6.

[4] Bhavanam A, Sastry RC. Biomass gasification processes in downdraft fixed bed reactors: a review. Chemical Eng Appl 2011;2. Num. 6.

[5] Buzzi-Ferraris G, Manenti F. BzzMath: library overview and recent advances in numerical methods. Comput Aided Chem Eng 2012;30(2):1312–6.

[6] Cáceres G, Anrique N, Girard A, Degrève J, Baeyens J, Zhang HL. Performance of molten salt solar power towers in Chile. J Renew Sustain Energy 2013;5: 053142. http://dx.doi.org/10.1063/1.4826883.

[7] Cucek L, Klemeš JJ, Kravanja Z. A review of footprint analysis tools for monitoring impacts on sustainability. J Clean Prod 2012;34:9–20.

[8] Demirbas A. Combustion characteristics of different biomass fuels. Prog Energy Combust Sci 2004;30:219–30.

[9] DOE (Department of Energy, USA), http://energy.gov/fe/science-innovation/clean-coal-research/gasification, [last accessed on 10.06.2014].

[10] Faravelli T, Frasssoldati A, Migliavacca G, Ranzi E. Detailed kinetic modeling of the thermal degradation of lignin. Biomass Bioenergy 2010;34(3):290–301.

[11] Gebreegziabher T, Oyedun AO, Hui CW. Optimum biomass drying for combustion – a modeling approach. Energy 2013;53:67–73.

[12] Hertwich EG, Zhang X. Concentrating-solar biomass gasification process for a 3rd generation biofuel. Environ Sci Technol 2009;43:4207–12.

[13] Ch Higman, Burgt VDM, Gasification. Elsivier Science; 2003. ISBN: 0750677074.

[14] Kitto JB, Stultz SC. STEAM: its generation and use. 41st ed. The Babcock & Wilcox Co.; 2005, ISBN 0963457012. USA.

[15] Klemeš JJ, Varbanov PS, Pierucci S, Huisingh D. Minimising emissions and energy wastage by improved industrial processes and integration of renewable energy. J Clean Prod 2010;18(9):843–7.

[16] Lam HL, Varbanov PS, Klemeš JJ. Optimisation of regional energy supply chains utilising renewables: P-graph approach. Comput Chem Eng 2010;34(5):782–92.

[17] Li H, Chen Q, Zhang X, Finney KN, Sharifi VN, Swithenbank J. Evaluation of a biomass drying process using waste heat from process industries: a case study. Appl Therm Eng 2012;35:71–80.

[18] Luo S, Guo X, Zhiquan Hu, Liu Sh, Maoyun He. Hydrogen-rich gas from catalytic steam gasification of biomass in a fixed bed reactor: influence of particle size on gasification particle. Hydrog Energy 2009;34:1260–4.

[19] Lv PM, Xiong ZH, Chang J, Wu CZ, Chen Y, Zhu JX. An experimental study on biomass air-steam gasification in a fluidized bed. Biosource Technol 2004;95: 95–101.

[20] Mettler MS, Vlachos DG, Dauenhauer PJ. Top ten fundamental challenges of biomass pyrolysis for biofuels. Energy Environ Sci 2012;5:7797–809.

[21] Miguel GS, Dominguez MP, Hernandez M, Sanz-Perez F. Characterization and potential application of solid particles produced at a biomass gasification plant. Biomass Bioenergy 2012;47:134–44.

[22] Pedroso DT, Machin EB, Silveria JL, Nemoto Y. Experimental study of bottom feed updraft gasifier. Renew Energy 2013;57:311–6.

[23] Perez JF, Meglar A, Benjumea PN. Effect of operating and design parameter on the gasification/combustion process of waste biomass in fixed bed downdraft reactors: an experimental study. Fuel 2012;96:487–96.

[24] Prins MJ, Ptasinski KJ, Janssen FJJ. From coal to biomass gasification: comparison of thermodynamic efficiencyvol. 32; 2007. p. 1248–59.

[25] Ranzi E, Couci A, Faravelli T, Frassoldati A, Migliavacca G, Pierucci S, et al. Chemical kinetics of biomass pyrolysis. Energy Fuels 2008;22:4292–300.

[26] Ranzi E, Corbetta M, Manenti F, Pierucci S. Kinetic modeling of the thermal degradation and combustion. Chem Eng Sci 2014;110:2–12.

[27] Ruiz JA, Juárez MC, Morales MP, Muñoz P, Mendívil MA. Biomass gasification for electricity generation: review of current technology barriers. Renew Sustain Energy Rev 2013;18:174–83.

[28] Sandeep K, Dasappa S. Oxy-Steam gasification of biomass for hydrogen rich syngas production using downdraft reactor configuration. Int J Energy 2013.

[29] Sinnott RK. Chemical engineering design. Coulson &Richardson's chemical engineering series; 2005. ISBN-13: 978-0750665384.

[30] Yang W, Ponzio A, Lucas C, Blasiak W. Performance analysis of a fixed-bed biomass gasifier using high-temperature air. Fuel Process Technol 2006;87: 235–45.

[31] Zhang HL, Baeyens J, Degrève J, Cacères G. Concentrated solar power plants: review and design methodology. Renew Sustain Energy Rev 2013;22:466–81.

[32] Siirola JJ, Edgar TF. Process energy systems: control, economic, and sustainability objectives. Comput Chem Eng 2012;47:134–44.

[33] Manenti F, Ravaghi-Ardebili Z. Dynamic simulation of concentrating solar power plant and two-tank direct thermal energy storage. Energy 2013;55: 89–97.

[34] Ranz WE, Marshall WR. Evaporation from drops, part I. Chem Eng Prog 1952;48:141–6.